IEEE Access
Multidisciplinary ⋮ Rapid Review ⋮ Open Access Journal

Received 10 March 2023, accepted 23 March 2023, date of publication 29 March 2023, date of current version 3 April 2023.

Digital Object Identifier 10.1109/ACCESS.2023.3262993

RESEARCH ARTICLE

Decentralized Demand Side Participation in Primary Frequency Control: Assessing the Impact of Response Rates

LEO CASASOLA-AIGNESBERGER AND SERGIO MARTÍNEZ, (Senior Member, IEEE)
Escuela Técnica Superior de Ingenieros Industriales, Universidad Politécnica de Madrid, 28006 Madrid, Spain

Corresponding author: Leo Casasola-Aignesberger (leo.casasola@upm.es)

This work was supported by the Spanish National Research Agency, Agencia Estatal de Investigación, under Grant PID2019-108966RB-I00/AEI/10.13039/501100011033.

ABSTRACT Increasing renewable energy generation is leading to reduced inertia in electric power systems. This challenges conventional frequency control methods, as frequency deviations become faster and more pronounced. One possible approach to maintaining system frequency within acceptable bounds is using demand-side response complementing current generation-side control strategies. However, evaluating the impact of different control strategies on frequency behavior is needed to compare their performance. This paper presents a set of conventional metrics and proposes a new metric for evaluating frequency behavior in electric power systems, based on a case study in an island power system in San Cristobal, Galapagos. Furthermore, it presents the impact on frequency of different demand-side response strategies that contribute to frequency control and their impact on the used batteries.

INDEX TERMS Ancillary services, decentralized control, demand response, primary frequency control, smart loads.

I. INTRODUCTION

Electrical power grid operation requires both frequency and voltage to remain within a tight range around their rated values. Conventional control strategies rely upon synchronous generators (SGs) to adjust either the excitation circuit or the mechanical power to compensate any deviation. While voltage is a local magnitude which is highly dependent on location, frequency is a global magnitude which can be measured at any point in the grid. This paper focuses on the issue of frequency deviations, which can be traced back to a real-time unbalance between power generation and demand. Renewable generation in electric power systems is usually interfaced with power converters [1] and does not offer inherent inertial response to frequency deviations. This leads to greater frequency deviations [2] and larger Rate of Change of Frequency (*RoCoF*) values, pushing existing frequency response services to their limits [3]. The frequency evolution over time is determined, for a given disturbance, by two distinct factors: the system's inertia, and the response of the control loops. The inertia is related to the kinetic energy of the rotating masses in turbines and synchronous generators of power plants, and directly influences the frequency behavior of the system right after the disturbance, before the control acts. Then, the response is determined by the control mechanisms of the power plant (typically vapor intake, water valve, or similar), and their dynamics. Their role is to restore the system into a generation-demand equilibrium and maintain the frequency at its rated value. The first instants after a disturbance, as stated above, are influenced by the systemB4s inertia. Therefore, the extreme *RoCoF* value that will be reached is given by the inertia present in the system (for a given disturbance) [4]. Limiting the *RoCoF* reduces, indirectly, the maximum frequency deviation, as it provides valuable time for the control mechanisms to act upon the generators. Furthermore, the increased frequency deviation and *RoCoF* values may compromise the stability of the system, as some protection devices depend on these magnitudes to keep the system in a safe operation range. Specifically, according to [5], the main issues can be sorted into:

The associate editor coordinating the review of this manuscript and approving it for publication was Salvatore Favuzza.

- Unintentional tripping of protections.
- Over extensive Load shedding.
- Frequency collapse before the tripping occurs.

Although this is out of the scope of this paper, in addition to frequency support, the protection concept might need to be revised. As the share of renewable generation grows in electrical power systems around the world, their ability to perform frequency control using conventional synchronous generators will decrease. Therefore, the ultimate goal of this study is to evaluate the ability of decentralized demand side response to contribute to frequency control in a future scenario where synchronous generators have been partially replaced by power electronics interfaced generation units. The limitations imposed on decentralized strategies, specifically the lack of knowledge about the system as a whole, poses new challenges: What is the appropriate rate of response? Can it be too high? Is it possible to set it automatically? How can it adapt to the changing circumstances of the system? These are some of the current open questions in this field, and this paper is a step towards an answer.

A. NON-CONVENTIONAL FREQUENCY REGULATION

To compensate this loss of inertia and allow the successful integration of renewable generation, several approaches can be used [6]:

1) *Distributed generation:* an adequate control of power converters can provide some frequency regulation even in small generation units, as in [7]. However, this approach is limited by the small energy reserve inherent to these units, the non-dispatchable nature of most renewable energy sources, and the large number of generation units due to their relatively small scale.
2) *Demand side response:* shifting the focus from generation to demand allows the provision of frequency regulation by modifying the demanded power in response to frequency deviations which, as stated above, can be measured locally. This contributes in the same way as conventional frequency control, but with the participation of many more units.
3) *Micro-grids:* a collection of controllable loads and distributed energy resources can cooperatively control the operation of the network, working in island mode [8]. Micro-grids usually incorporate some sort of energy storage capacity, which plays a key role in both energy management and frequency regulation [9].

This paper focuses on load participation for frequency control purposes, which will be discussed briefly to summarize the context in which this study has taken place.

B. DEMAND SIDE PARTICIPATION

In principle, any load could potentially take part in frequency control, as long as its power consumption can be regulated and its response time is sufficiently small. The loads more commonly found in literature are either of thermal nature [10], [11], [12], [13] or electric vehicles [14]. Thermal loads have large time constants compared to electromechanical transients, and therefore brief power fluctuations do not have a significant impact in their intended use. Furthermore, thermal loads constitute a sizable portion of energy demand in most power systems. Electric vehicles, on the other hand, allow precise power control, have inherent energy storage capabilities, and are always interfaced by a power converter. Although not yet as prevalent, their presence in electric power systems is expected to grow in the close future [15].

Regarding the control of the loads taking part in frequency regulation, three categories can be established according to the decision-making process: centralized, decentralized and distributed control.

1) *Centralized control:* a single unit measures the system frequency, calculates the appropriate response and sends individual control signals to each load, which adjust the power demand accordingly. As this allows to take into consideration information about the whole system and implement a global optimization algorithm, accurate frequency response and control can be achieved by this control scheme. The main drawback, on the other hand, is the need of robust and reliable communication channels capable of transmitting large quantities of information in real time. This comes at a significant cost, is exposed to various cyber-threats and can suffer from time-delays [16] or communication interruptions. Research with this approach includes [9], where a micro-grid is regulated using an external energy reserve.
2) *Decentralized control:* each load decides what response is adequate for the current situation based only on locally available measurements. Reference [14] studies a small islanded power system (as we do in this paper) under sharp load variations and analyzes the contribution to frequency regulation of plug-in hybrid electric vehicles. This control strategy does not require any communication and is therefore not exposed to the centralized control drawbacks. However, for the same reason, the overall state of the system is unknown to any single actor and no global optimization is possible.
3) *Distributed control:* sort of a combination of the previous two, can be implemented in different ways. For example, load aggregators controlling multiple loads in a centralized way or a single control center which fixes the set-points and lets the individual loads adjust their responses based on local measurements. This approach reduces the communication needs of the control center while still retaining some potential for optimization, although not on a global scale. Moreover, it remains vulnerable to communication problems. A good example of this is [17], as it splits the response into low and high frequency components, allocating them to appropriate elements in the grid. Other examples are [10], [18], where the set-points of thermal loads are fixed centrally and each unit responds on its own, or [19], which proposes a Fuzzy Synthetic Inertia Control to

optimize the Fast Frequency Response in low-inertia microgrids.

This paper addresses decentralized demand side participation in primary frequency control, where only local measurements are available to adapt the demand side response to frequency deviations. Particularly, this work presents a selection of conventional metrics and proposes a new one to quantitatively compare the performance of frequency control strategies. Assessing the frequency behavior is crucial for the demand response to adequately contribute to frequency control. The proposed metric consists of a single numerical value, so that two different scenarios can be directly compared and evaluated.

Expanding on previous work, focused on identifying ways of providing frequency response with load aggregation [20] and from the generation side [21], this work analyzes the impact load response has on system frequency. Further work includes [22], which proposes the use of controlled domestic heat pumps to provide frequency support, or [23], where a combination of refrigerators and Flywheel Energy Storage Systems is used and includes an estimation of the economic benefit. It has to be noted that, unlike synchronous generators, which inherently respond to frequency deviations, demand side response requires the frequency to be actively measured and, therefore, current knowledge about the system behavior, modeling and control strategies have to be revised [24].

Further classification of Demand Response is summarized in [25], which divides the possible programs into ''Incentive based'' and ''Time-based''. It also states that, while some time-based programs can admit user intervention, ancillary services, such as the frequency control support proposed in this paper, must happen automatically because of the need for a fast response. Reference [26] classifies according to the business model, but the management of the economical aspect of these programs is yet to be settled and it is out of the scope of this paper.

The rest of this paper is structured as follows: section II presents the model of a power system in an island, as a case study; section III describes the scenarios that have been considered; section IV describes the metrics used and develops the new proposed metric; section V presents the results and provides a brief discussion on the limits for this type of control; section VI presents the impact of the developed strategies on the used batteries; and section VII concludes the paper.

II. SYSTEM AND MODEL

The electric power system of the island of San Cristobal, in Galapagos, Ecuador, has been chosen as a benchmark for this study, as it is a small system which incorporates high levels of wind power generation. It consists of synchronous generation and a wind farm, connected to the main consumption bus by a 12 km long line. Figure 1 presents the diagram of the main components of the electric power system, as it has been implemented in the model. It represents the main components: the synchronous generator and the wind turbines as generators, connected by transformers to the main bus. The considered load combines impedance load, asynchronous motor load and dynamic power load. The *Specialized Power Systems* library in *Matlab/Simulink* [27] has been chosen as the platform for the implementation of the model, performing discrete electromechanical simulations with a step time of 50 μs. The model used for each element is detailed at the end of each description in the following subsections. A more detailed description of this electrical power system, including relevant parameters, is available in [28].

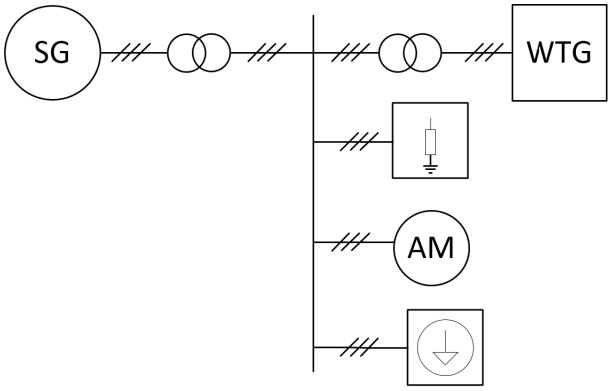

FIGURE 1. Diagram of the simulated power system.

A. SYNCHRONOUS GENERATORS

Three 813 kVA synchronous generators, coupled to diesel engines, are available for power generation. In its current form, the power system operation is carried out by the synchronous generators for both frequency and voltage control. This paper proposes a way of supporting the frequency control carried out by the synchronous generators. While it cannot be a replacement, it does allow more renewable energy to be integrated into the generation mix, therefore reducing the use of fossil fuels. Parameters for the engine, the generator and the governor are taken from [28].

The synchronous generator has been implemented using the ''Synchronous Machine, pu Standard'' and ''Excitation System'' blocks provided by the *Specialized Power Systems* library.

B. WIND FARM

The wind farm in San Cristobal consists of three 800 kW wind turbines, which can be independently turned off if necessary, and are assumed to operate at unity power factor. These wind turbines are located close to each other, roughly aligned on an east-west axis without any major obstacles that could cause wind disturbances. The wind profile incident to each of them is assumed to be the same, but delayed with respect to the previous wind turbine by

$$t = \frac{125(m)}{U(m/s)} \times sin(\phi) \tag{1}$$

where U is the average wind speed for that wind profile and ϕ is the angle of incidence. Trying to obtain a realistic power output from the wind farm, where the wind does not reach all turbines at the exact same time, this angle is kept constant at $\phi = \frac{\pi}{4}$ for this study.

The power fluctuations due to the varying wind speed in the wind profile are the cause of the frequency fluctuations that are addressed in this paper.

The wind turbine generators have been implemented using the "DFIG Wind Turbine" block, provided by the *Specialized Power Systems* library.

C. LOADS

The load in any electric power system is diverse, and may have diverse responses to both frequency and voltage deviations. For modeling purposes, two categories have been established:

1) CONVENTIONAL LOAD

Conventional loads do not actively take part in frequency control, but may have a natural response to frequency or voltage deviations. Conventional load has been modeled as a combination of three types:

- **Constant power loads**. They demand a constant active power and operate at unity power factor. These loads are undisturbed by frequency or voltage deviations.
- **Constant impedance loads**. They naturally respond to voltage deviations, but are almost insensible to frequency deviations.
- **Inertial loads**. They have a certain amount of energy stored in the form of kinetic energy and respond to both frequency and voltage deviations. They have been modeled as a half loaded equivalent asynchronous motor, with an inertia constant of 0.5 s over a given rated power S_{AM}.

Each of these categories absorb about a third of the total demanded power. These loads have been implemented using the blocks "Three-Phase Dynamic Load" with constant power demand, "Three-Phase Series RLC Load" with constant parameters and "Asynchronous Machine pu Units" with constant torque, respectively.

2) FREQUENCY RESPONSIVE LOAD

Frequency responsive loads take part in frequency control by actively adapting its power demand to frequency deviations. This kind of load is assumed to consist of electric vehicles connected to the grid in idle mode (not actively charging), capable of responding to the control signal both absorbing and providing active power. This type of load has been implemented in the model by a "Three-Phase Dynamic Load" block, where the power is dynamically adjusted.

Incorporating demand side response into frequency regulation requires adapting the equipment to the newly required behavior. A decentralized approach requires no further infrastructure, avoiding significant investment: the control signal has to be set based on locally available measurements. The frequency signal is obtained by a Phase-Locked-Loop (PLL) and filtered with a time constant of 0.1 s in order to avoid fast frequency oscillations due to excessive response, as presented in [29]. This signal is then incorporated into the frequency sensitive response and sets the power demand to the desired value. As the element taking part in power demand/injection is a power electronics interfaced battery, it is safe to assume that its response is fast and accurate to adjust to any value within its power limits.

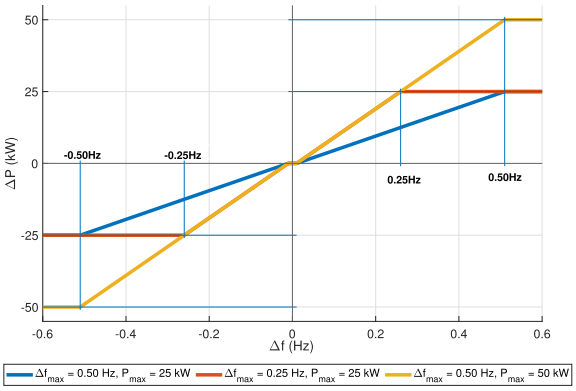

FIGURE 2. Example of theoretical $\Delta f - \Delta P$ curves for different values of Δf_{max} and ΔP_{max}.

The load's response to frequency deviations can be characterized by the amount of power that can be involved, and the rate at which it responds, measured in W/Hz. For a given load, with a certain power rating, the response rate can be set through the frequency deviation value (Δf_{max}) for which it will provide its maximum power (ΔP_{max}), as seen in figure 2 for three different cases. This value has to be tuned to obtain the best possible performance and will be the main topic of this paper.

However, different combinations of Δf_{max} and ΔP_{max} can result in the same slope. Figure 2 shows that case: having 50 kW with a $\Delta f_{max} = 0.50$ Hz provides the same response as having 25 kW with a $\Delta f_{max} = 0.25$ Hz, as long as the maximum power is not reached. On the other hand, if 25 kW are available and Δf_{max} is set to those same 0.50 Hz, the response rate drops to half the slope. The frequency response of this active load is therefore a combination of a tunable parameter (Δf_{max}) and the total amount of demand that is available, which cannot be imposed.

The behavior of the frequency responsive loads differs slightly from the graph shown in figure 2 because of the presence of the filter in the frequency measurement. That filter will slightly delay the action of the controller, accounting for any delays that may happen in a real unit, and leads to slight deviations in the $\Delta P - \Delta f$ responses, as shown in figure 3a. While the ideal response would be the straight line shown in red in figure 3a, the recorded response is a cloud of points around that line, represented in blue. Figure 3b, is a close-up view of figure 3a. It shows, for each instant, the recorded $\Delta P - frequency$ pairs (blue points). These might differ from

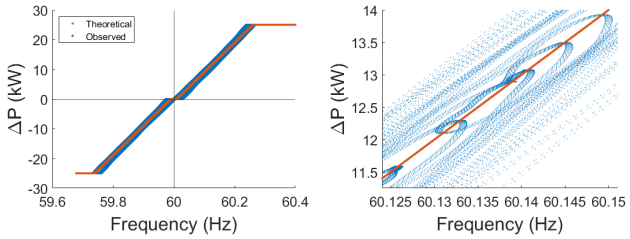

(a) General overview. (b) Zoom of figure 3a.

FIGURE 3. Example of the observed $\Delta P - \Delta f$ behavior for the case with $\Delta P_{max} = 25$ kW, $\Delta f_{max} = 0.25$ Hz and wind profile w_B.

the set-points imposed by the control (red line) because of the response's dynamics.

As the average frequency deviation must be kept close to zero, and power deviations in opposite directions compensate the energy exchange, the net impact on users is not significant, as discussed in section VI. Nevertheless, a proper incentive and retribution scheme should be developed to compensate the use of the equipment, its devaluation and the service provided to the power grid. However, the economic implications deserve a more detailed study, which exceeds the scope of this paper.

III. SCENARIOS

The simulations carried out in this study focus on the frequency deviations caused by wind speed variability in a small power system, and the ability of frequency responsive loads to partially compensate the power unbalance and reduce the frequency deviations. The conceptual map is shown in figure 4: the wind profile, with its wind speed variability, injects some (variable) power into the electric power system. This causes frequency deviations, that are detected by part of the load, which adjusts its power demand accordingly.

To analyze the impact of demand side participation in frequency regulation and the effect of different rates of response to frequency deviations, two scenarios have been considered with different wind profiles (w_A and w_B). The goal is to evaluate the frequency behavior of the electric power system under two kinds of wind profiles: one where the wind is quite constant (w_A), and another one with significant variability (w_B). Therefore, both wind profiles have similar average wind speeds (U) of about 5 m/s, so that the average power output is similar, but they differ in variability, measured as the Turbulent Index (TI) according to the definition of [30], source of this data. Table 1 summarizes the main values for the wind profile used.

In order to consider the worst case, all three wind turbines are assumed to be online, and a single synchronous generator provides the remaining power generation (roughly half of the demand) and, in the base case, all the frequency regulation. The total demand is about 400 kW, divided into 150 kW of asynchronous motor, 150 kW of constant impedance load and 100 kW of constant power load.

Along with the wind profiles, two more parameters are modified to establish all the scenarios to be simulated: the

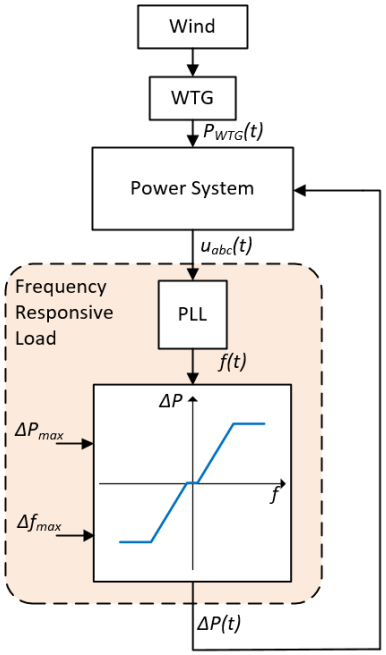

FIGURE 4. Simulation set-up.

TABLE 1. Wind data parameters.

Magnitude	Symbol (units)	w_A	w_B
Mean	$U\ (m/s)$	5.25	4.61
Standard deviation	$SD\ (m/s)$	0.1181	0.4973
Turbulent index	$TI\ (\%)$	2.25	10.80
Min. value	$U_{min}\ (m/s)$	4.84	2.77
Max. value	$U_{max}\ (m/s)$	5.68	6.23

TABLE 2. Parameters for the studied scenarios.

Parameter	Values
Δf_{max} (Hz)	0.125, 0.25, 0.375, 0.50
ΔP_{max} (kW)	6.25, 12.5 25, 50, 75, 100

amount of demand that takes part in frequency regulation and the rate at which it does so, characterized by its Δf_{max}. A wide range of power values has been chosen, from 6.25 kW up to 100 kW, with Δf_{max} ranging from 0.125 Hz to 0.50 Hz in all cases, summarized in table 2. Therefore, 50 cases have been considered: 2 base cases (without demand side participation in frequency regulation) and 48 different combinations of two wind profiles, six power values and four Δf_{max} values.

IV. METRICS

This section presents the metrics used to evaluate the frequency behavior based on the base case, with no demand side participation in frequency control. Afterward, the results for the cases with increasing demand side participation will be presented in section V, using the previous metrics to evaluate the performance of the proposed method and detect possible excess of response.

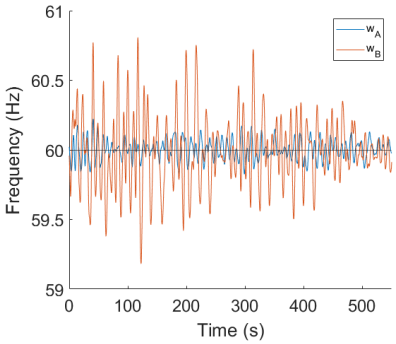

FIGURE 5. Frequency evolution for the base cases.

In the base cases, as presented in section III, no demand side response takes active part in frequency regulation, and only the synchronous generator provides frequency control. Conventional loads may respond naturally to frequency deviations, as in the case of the asynchronous motor.

The frequency behavior in these cases is presented in figure 5. It shows that, as expected, the frequency behavior for the steadier wind profile w_A presents less frequency deviations than w_B, with more wind speed variability. In this section, a series of metrics are presented which allow to evaluate the severity of the frequency deviations and therefore help compare the different scenarios quantitatively. The numerical results for all the metrics used are summarized later in table 4, according to the definitions given below.

A. EXTREME VALUES

The first metric that can be used is the extreme values reached in the period under study. That is, the maximum and minimum frequency values (f_{max}, f_{min}), along with the maximum amplitude of the frequency deviations, defined as the difference between these extreme values, as expressed in equation 2:

$$\Delta f_{amp} = f_{max} - f_{min} \tag{2}$$

Under ideal circumstances, where the frequency stays at its rated value, this metric would be zero, and it can obviously be only non-negative, so greater values mean a worse behavior of the system frequency and a worse performance of the frequency control.

B. VARIABILITY

The second metric that is evaluated is the variability of the frequency, measured as the standard deviation of the frequency, f_{SD}, and the mean absolute deviation, f_{mad}, as defined in equation 3.

$$f_{mad} = mean(|f(t) - f_m|) \tag{3}$$

where $f(t)$ is the frequency and f_m its mean value, usually close to the rated value, in this case 60 Hz. Under ideal circumstances, both these metrics would be zero, and can only be non-negative, so greater values indicate a worse performance.

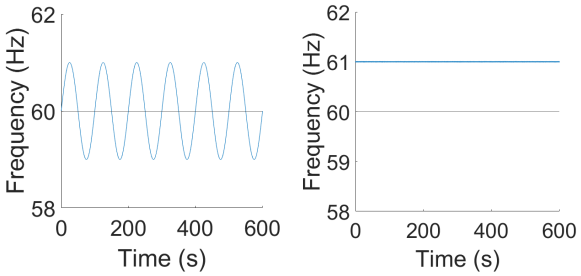

(a) Slow and large variations. (b) Fast but small variations.

FIGURE 6. Synthetic frequencies for metrics evaluation.

TABLE 3. Values of the different metrics for the two synthetic scenarios.

Case	Δf_{amp}	f_{SD}	f_{mad}	$RoCoF_{rms}$	Proposed
1	2 Hz	0.7 Hz	0.6 Hz	0.04 Hz/s	0.63
2	20 mHz	7 mHz	6 mHz	4 Hz/s	0.99

1) RATE OF CHANGE OF FREQUENCY (RoCoF)

The third metric that is considered is the rate at which the frequency changes over time, also known as *Rate of Change of Frequency*. Obviously, a *RoCoF* value exists for each instant in time. These values have to be summarized in some way to evaluate the performance. The extreme values ($RoCoF_{min}$, $RoCoF_{max}$) and its quadratic mean (or root mean square, *rms*) have been chosen and are included in table 4.

C. PROPOSED METRIC

The aim of this metric is to easily compare the performance of different frequency control algorithms. This cannot be done by the other analyzed metrics, as the following examples show. Two synthetic frequencies will be presented, to support our case, both of them unacceptable in any electric power system for different reasons:

1) The first case is a slow (1/100 Hz) but significant (1 Hz amplitude) variation around the rated value of 60 Hz.
2) The second case is a rapid (100 Hz) but small (0.01 Hz amplitude) oscillation around 61 Hz, so 1 Hz above the rated value.

Figure 6 shows the graphs of both cases over a time period of 600 s. The first case would be labeled unacceptable by the extreme values metric, as well as by the variance metrics (Δf_{amp}, f_{SD} and f_{mad}), while acceptable by any of the *RoCoF* metrics. The opposite is true for the second case. The values for these metrics are shown in table 3.

Therefore, none of the previous metrics alone is able to provide an acceptable evaluation on the performance of the frequency behavior. In contrast, the new proposed metric rates both cases as badly behaved, assigning a value of the same order of magnitude. The aim is to condense the information about the performance into one single numerical value, so that it can be used to evaluate the performance of the frequency control system and take further action if needed. The calculation method for this new metric is exposed below.

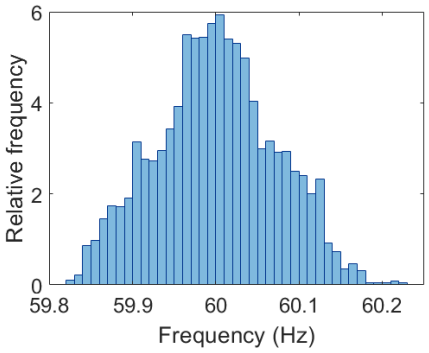

FIGURE 7. Histogram for the base case with wind profile w_A.

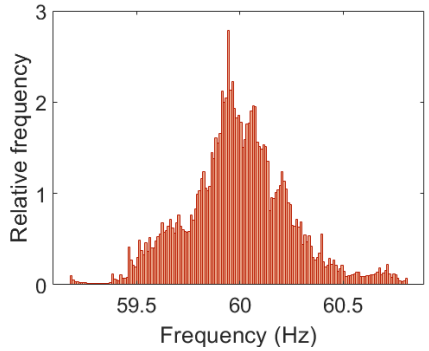

FIGURE 8. Histogram for the base case with wind profile w_B.

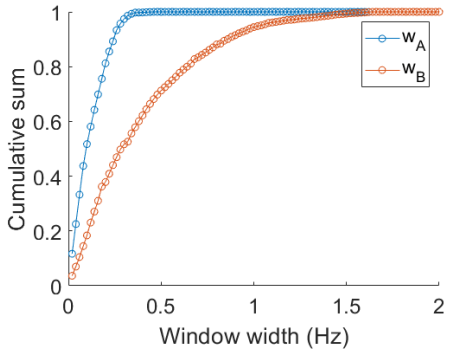

FIGURE 9. Cumulative sum of increasing window width.

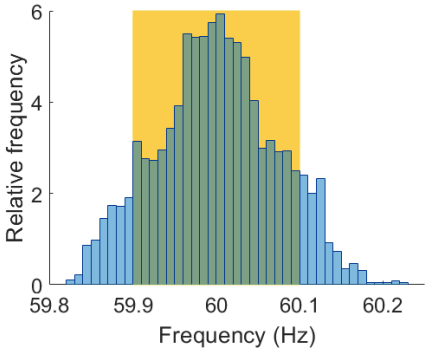

FIGURE 10. Histogram for the base case with wind profile w_A. The shaded area marks the interval 60 ± 0.1 Hz. The sum of the bins inside this interval defines the point corresponding to a window width of 0.2 Hz in the blue curve of figure 9.

This new metric, the fourth and last metric used, is related to the relative distribution of the frequency values. In an ideal scenario, the only measurement would be the rated frequency, 60 Hz in this system. If the frequency values are represented in a histogram, such as figures 7 and 8, it is clear that the frequency samples are gathered around the rated frequency. The sum of the bins around the rated frequency is a measure of the performance of the frequency control, assuming all other factors are kept constant. In figure 8, a slight bimodal behavior is observed, as explained in [31]. The values have been normalized in such a way that the total area of all the bins is equal to one.

To quantify this, the bins inside windows of increasing width and centered at 60 Hz are summed, generating the cumulative sum curves represented in figure 9. An example of the calculation of a single point in one of these curves is shown in figure 10. To make sure all data points are considered, the width of the windows ranges up to 2 Hz. The minimum considered width is set equal to the dead band of the demand response, 20 mHz. Increments of 10 mHz in each direction have been taken to generate figure 9. These curves are very illustrative but they do not allow a direct comparison between cases because they do not consist of a single numerical value.

To overcome this limitation, the area between the curve and the value $y = 1$ is calculated, as presented in figure 11. Once again, if the frequency did not have any deviations, this value would be zero, and greater values represent a worse performance of the frequency regulation systems. For a given situation, the performance of different frequency control strategies can be evaluated by comparing their respective values.

V. RESULTS

In this section, the results obtained for the enhanced response scenarios will be analyzed, as presented in section III. It evaluates the impact demand side participation can have on frequency behavior. To do so, the system is exposed to the same two wind profiles, with different amounts of demand (ΔP_{max}) taking part in frequency control, as well as different response rates to frequency deviation (Δf_{max}). Only the cases with the same amount of ΔP_{max} can be compared, as we are trying to evaluate the impact different response rates have on system frequency.

A. LOW VARIABILITY WIND PROFILE

The low variance wind speed scenario (w_A) gives a worse insight into the effect of demand side participation in frequency control, because the frequency is relatively well behaved in the base case. Figure 12 shows how the frequency deviation amplitude decreases in all cases with low wind speed variability with increasing ΔP_{max} and Δf_{max}.

As shown in figures 13, 14 and 15, the standard deviation, the mean absolute value, and the proposed metric improve with decreasing Δf_{max} under these circumstances. It is also

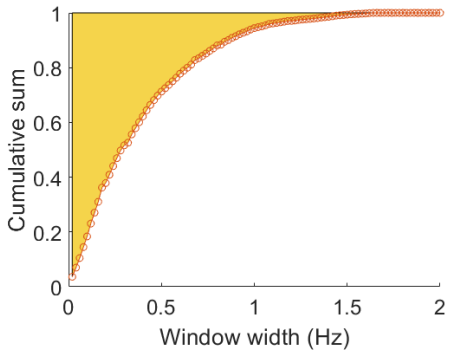

FIGURE 11. Area above the curve for w_B, which is the numerical value used as a metric of frequency behavior.

TABLE 4. Frequency results for the base cases in both wind scenarios.

	Low variability (w_A)	High variability (w_B)
$\Delta f_{amp}(Hz)$	0.3973	1.6257
$f_{SD}(mHz)$	72.0328	252.1493
$f_{mad}(mHz)$	57.9125	191.6640
$RoCoF_{min}(mHz/s)$	−182.8337	−473.4838
$RoCoF_{max}(mHz/s)$	150.0302	479.9909
$RoCoF_{rms}(mHz/s)$	47.3647	152.1125
Proposed metric	0.052995	0.18664

clear that all cases improve over the base case. These results also indicate that, with lower ΔP_{max} available, a reduction in Δf_{max} leads to greater improvement than with high levels of available ΔP_{max}. For example, in figure 15, going from $\Delta f_{max} = 0.25\ Hz$ to $\Delta f_{max} = 0.125\ Hz$ has very little effect on the metric when 100 kW are available for frequency control, but a more significant effect when only 6.25 kW are available. Finally, figure 16 summarizes the extreme $RoCoF$ values for these cases and, according to this metric, the improvement obtained by decreasing Δf_{max} is also greater when less ΔP_{max} is available.

B. HIGH VARIABILITY WIND PROFILE

On the other hand, the high variance wind speed scenario (w_B) gives a good insight into the effect of demand side participation in frequency control, as the wind speed variations induce significant frequency deviations that can be mitigated from the demand side.

These results show that, in general, having more demand side participation in frequency control yields a better overall performance, regardless of the metric used to evaluate frequency behavior. However, for a given available power in demand side participation, setting the appropriate value for its response rate is not straightforward, as it depends on the power deviations (in the analyzed cases induced by wind speed fluctuations), the amount of available power to provide frequency control, and the metric used for frequency behavior evaluation. For example, if f_{SD} or f_{mad} are used as the evaluation metrics, the behavior improves with increasing response rate (and therefore decreasing Δf_{max}), regardless of wind profile and available power, as seen in figures 17 and 18. On the other hand, if the evaluation metric is Δf_{amp}, an interesting behavior emerges: under some circumstances, increasing the

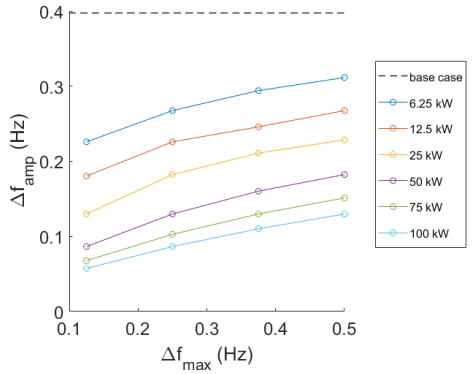

FIGURE 12. Maximum frequency deviation amplitude (Δf_{amp}) for all cases with low wind speed variability (w_A).

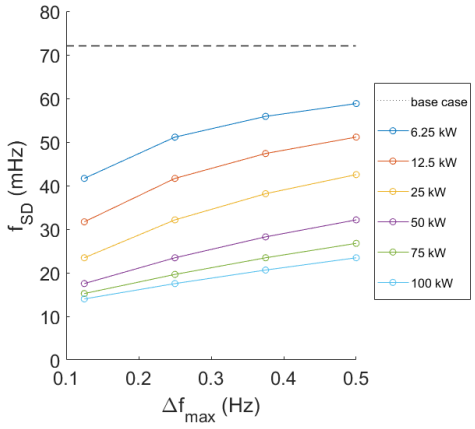

FIGURE 13. Frequency standard deviation (f_{SD}) for all scenarios with low wind speed variability (w_A).

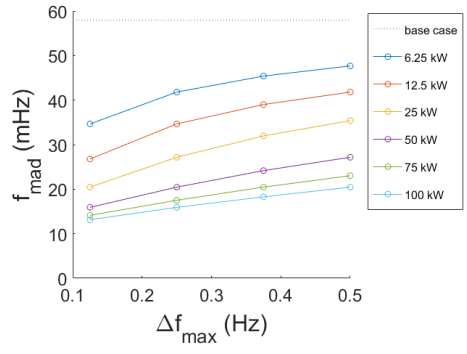

FIGURE 14. Mean absolute deviation (f_{mad}) for all scenarios with low variability wind profile w_A.

response rate can lead to worse performance. This can be seen in figure 19, which shows Δf_{amp} in the cases with high variability wind profile: with insufficient ΔP_{max}, Δf_{amp} does not decrease as Δf_{max} decreases, but rather stays the same or even increases again for some cases. For scenarios with less available power, if Δf_{max} is set to a low value, ΔP_{max} can be easily reached, leaving the system without further demand side response capabilities for frequency regulation. If under

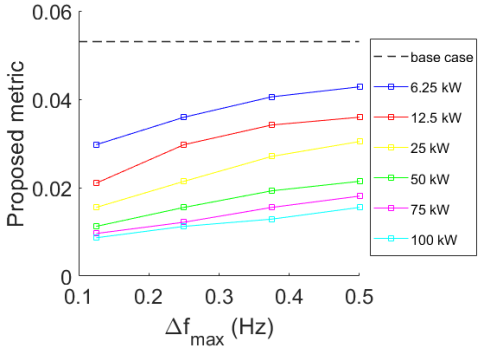

FIGURE 15. Proposed metric for the cases with low wind speed variability (w_A).

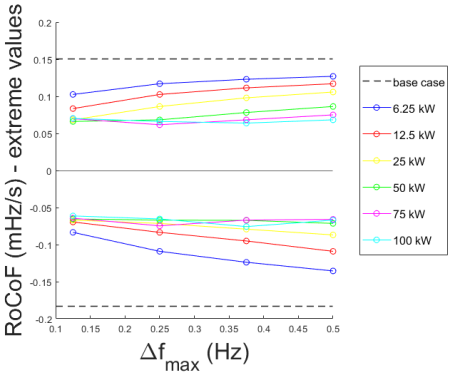

FIGURE 16. Extreme *RoCoF* values for the low variability wind profile w_A.

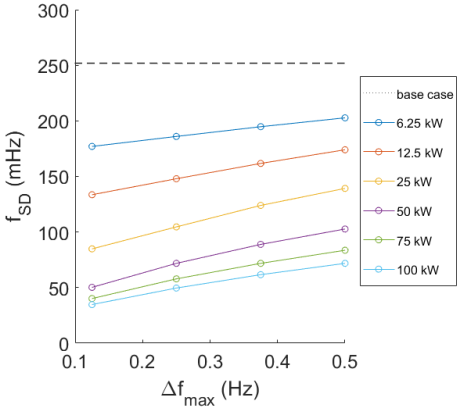

FIGURE 17. Frequency standard deviation (f_{SD}) for all scenarios with high wind speed variability (w_B).

these circumstances a severe wind gust appears, it can lead to high frequency deviations.

Figure 20 shows that, in these cases, if the performance is measured with the proposed metric, the frequency behavior improves in all cases with lower values of Δf_{max}. An example of the curves that give rise to this metric is shown in figure 21. This figure shows that the cumulative sum grows faster for smaller values of Δf_{max}, leaving them to the left of the base case. Furthermore, the smaller the value of Δf_{max}, the faster the cumulative sum grows. In figure 20 it is noteworthy that, for high and low values of ΔP_{max}, the influence of Δf_{max}

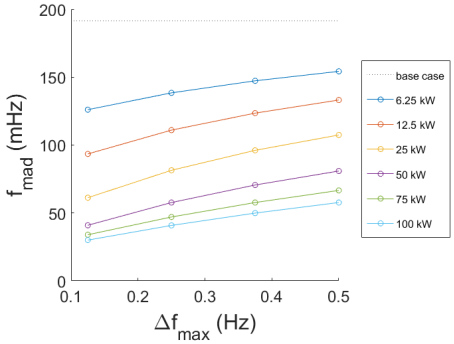

FIGURE 18. Mean absolute deviation (f_{mad}) for all scenarios with high variability wind profile w_B.

is less than for intermediate values of ΔP_{max}. In addition to that, the *RoCoF* values summarized in figure 22 show a behavior similar to the extreme values of frequency in figure 19: with enough available ΔP_{max}, the performance improves with decreasing Δf_{max}, but an excessive response rate can be counterproductive. This can be clearly seen in figure 19: for this metric (Δf_{amp}), the frequency behavior for the case with $\Delta P_{max} = 25\ kW$ improves when Δf_{max} is reduced from 0.5 Hz to 0.375 Hz, but gets worse when further decreased to 0.125 Hz. A similar behavior can be seen in figure 22, for the cases with $\Delta P_{max} = 25\ kW$ and $\Delta P_{max} = 12.5\ kW$.

C. COMPARISON

Finally, a brief comparison of the cases studied for the two different wind profiles is presented. The first aspect to notice is that the same system is analyzed under two distinct scenarios: one where the wind speed presents small variance (w_A) and another one where the wind profile presents a high variance (w_B). With no demand side participation in frequency control (base case), the frequency behavior of the system in both scenarios is shown in figure 5. It shows larger frequency deviations under wind profile w_B than under wind profile w_A. This is clearly reflected in the histograms of both cases, shown in figures 7 and 8, where the frequency under scenario w_B is much wider spread than the frequency under scenario w_A.

The dispersion can be measured as the amplitude of the frequency deviations (Δf_{amp}), shown in figures 12 and 19. They show that any presence of frequency responsive loads improves the frequency behavior of the system. Under highly variable wind conditions (w_B), a proper load response can reduce the Δf_{amp} values to those seen in better wind conditions without load response (w_A base case).

The w_A scenario, with low wind variability, presents the expected behavior: more available power with more aggressive response leads to less frequency deviations. However, the w_B scenario presents a somewhat different behavior: the intermediate power cases (12.5 kW and 25 kW) present a minimum of Δf_{amp} for intermediate values of Δf_{max}. It is not clear what causes this behavior, but it is suspected that,

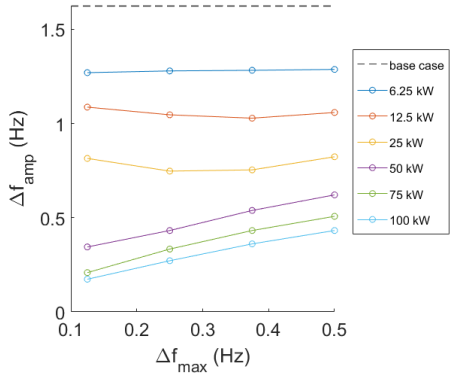

FIGURE 19. Maximum frequency deviation amplitude (Δf_{amp}) for all cases with high wind speed variability (w_B).

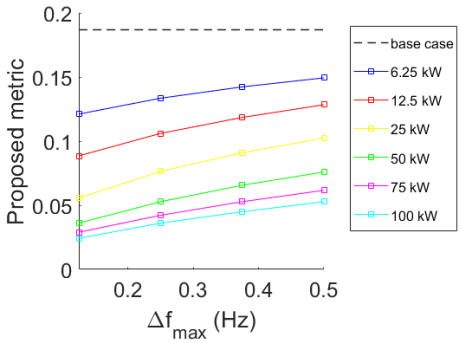

FIGURE 20. Proposed metric for the cases with high wind speed variability (w_B).

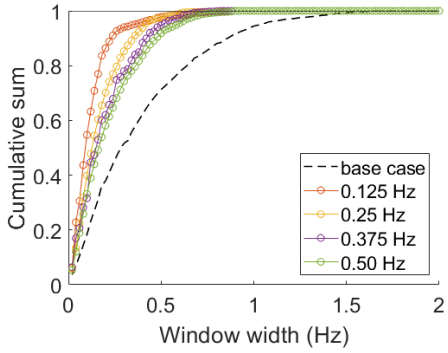

FIGURE 21. Cumulative sum of increasing window width, for the w_B scenario with 25 kW of demand taking part in frequency control.

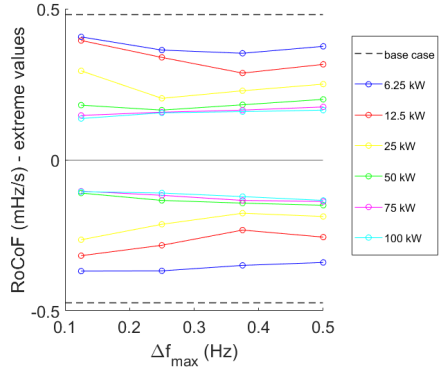

FIGURE 22. Extreme *RoCoF* values for the high variability wind profile w_B.

at specific points in time, a sudden change in wind speed occurs while the load response capacity is already saturated. At higher Δf_{max} values the response is not yet saturated.

When evaluating the frequency behavior with a variability metric (f_{SD} or f_{mad}), the situation changes because these metrics are not as susceptible as Δf_{amp} to extreme but singular values. All these cases show a similar behavior, a reduction of Δf_{max} decreases the value of the metric. Figures 13, 14, 17 and 18, show that achieving values similar to the w_A base case is possible with sufficient power and an adequate response rate.

If the evaluation is carried out by using the new developed metric, as shown in figures 15 and 20, the conclusions are similar to those based on the variance metrics: any presence of frequency response improves the frequency behavior, increasing response rates is beneficial (in general) and the values of the base case with w_A are achievable with sufficient ΔP_{max} and appropriate response rates.

Finally, the extreme *RoCoF* metric shown in figures 16 and 22 presents a similar behavior as observed with the Δf_{amp} metric, as both are sensible to singular extreme values.

Therefore, it can be concluded that the proposed metric properly captures the frequency behavior of the power system, with the potential of detecting steady-state frequency deviations which would not be captured by the other presented metrics.

VI. DISCUSSION

From the results presented in section V, it seems that higher available demand side participation alongside the lowest possible Δf_{max} yields the best performance. However, as previously shown, an excessive response rate may lead to greater Δf_{amp} than a moderate response under some circumstances. Concerning the available power, it cannot be fixed by the designer, as it depends on the amount of consumers that are willing to participate. Regarding this matter, more seems to be better, not only because it improves the overall performance, but because it also allows the burden to be shared among more actors and, therefore, decreases the stress that each of them support.

To evaluate the impact on the consumer side, a second series of metrics have been considered regarding the power profile participating in frequency control.

It is possible to provide frequency support in various ways [32]: from dedicated energy storage devices (such as batteries, flywheels or similar) to frequency sensitive consumers. The latter case depends on some sort of energy storage to reduce the impact that the final consumer suffers due to the power deviations required to support frequency control. In the case of thermal-electric loads (heat-pumps, water heaters, air-conditioning units, refrigerators and similar appliances), the thermal inertia of the system (relatively slow compared to the frequency dynamics) is enough to absorb these fluctuations, such as proposed in [33]. In the case of connected EVs, as the electronic-interface allows a fine controlfor whatever

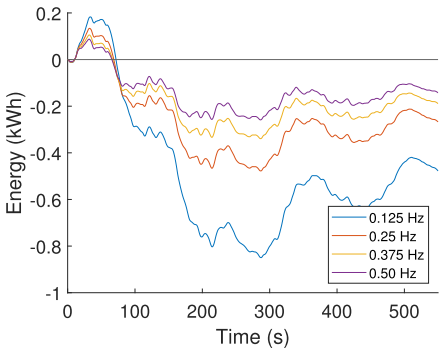

FIGURE 23. Evolution of energy exchange in the worst case: a 100 kW load with the w_B wind profile.

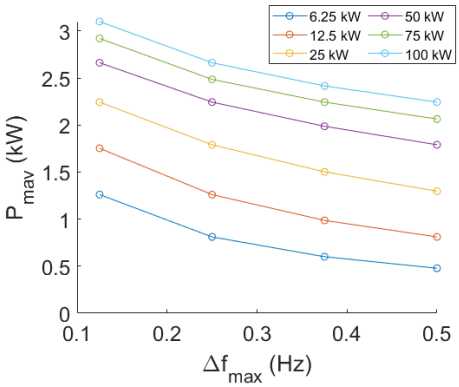

FIGURE 24. Mean absolute value of the power provided by the batteries in the scenarios with low wind variability (w_A).

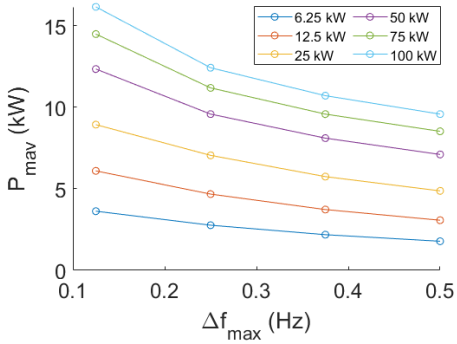

FIGURE 25. Mean absolute value of the power provided by the batteries in the scenarios with high wind variability (w_B).

TABLE 5. Results for P_{mav} (kW) in w_A scenarios for all combinations of ΔP_{max} and Δf_{max}.

	0.125 Hz	0.25 Hz	0.375 Hz	0.50 Hz
6.25 kW	1.2612	0.81115	0.6005	0.4779
12.5 kW	1.7531	1.2612	0.9865	0.81115
25 kW	2.2439	1.7906	1.5030	1.2971
50 kW	2.6627	2.2439	1.9873	1.7906
75 kW	2.9209	2.4857	2.2439	2.0644
100 kW	3.1007	2.6627	2.4159	2.2439

TABLE 6. Results for P_{mav} (kW) in w_B scenarios for all combinations of ΔP_{max} and Δf_{max}.

	0.125 Hz	0.25 Hz	0.375 Hz	0.50 Hz
6.25 kW	3.6294	2.7694	2.1883	1.7848
12.5 kW	6.1036	4.6789	3.7307	3.0740
25 kW	8.9414	7.0560	5.7519	4.8768
50 kW	12.354	9.5882	8.1132	7.1105
75 kW	14.498	11.195	9.5881	8.5314
100 kW	16.168	12.433	10.719	9.5881

regime is desired, it is possible to adjust their power to the system's requirements, providing a frequency sensitive load and using the internal battery as provisional energy storage. For this study, this energy storage is assumed to consist of batteries that are not active (nor charging or discharging) but are plugged-in, for example, connected electric vehicles in idle mode.

To assess the impact on the load, the maximum (P_{max}), minimum (P_{min}) and mean (P_{mean}) power demand are considered, as well as the mean absolute value (P_{mav}), which is a measure of the total energy exchanged by the battery.

The first noticeable detail that should be pointed out is the fact that, depending on the scenario, the demand response can be saturated, which leaves the system without demand side support for further disturbances, with consequences already presented in section V of this paper. Another important reading is that the mean power exchange is small, which means the impact on the final battery state of charge is also small. As can be seen in figure 23, the amount of energy exchanged, stays close to zero during the whole simulation, especially when compared to the involved power rating.

The last metric used involves the power provided by these batteries and its integral over time. If the power is integrated, the results represent the energetic impact frequency control has had on the battery, how much it has been charged or discharged. However, this does not represent the whole impact. According to [34], battery degradation is closely related, among other factors, to the total amount of energy that passes through the battery, regardless of its direction (charging or discharging). Therefore, the *mean absolute value* (P_{mav}) for each scenario is directly related to the degradation the battery suffers from participating in frequency control under these specific circumstances. Tables 5 and 6 summarize the numerical values for all studied scenarios.

Figures 24 and 25 present the values of P_{mav} for each scenario, and it can be seen that, in all cases, decreasing Δf_{max} leads to a higher value of P_{mav} and therefore greater battery degradation. This behavior is expected: as the value of Δf_{max} increases, the response to a certain frequency deviation decreases in power (see Fig. 2).

Comparing battery degradation in scenarios with different amounts of ΔP_{max} is not the goal of this paper. However, one must say that this comparison is to be done carefully. It is safe to assume that, with more power available, the total battery capacity would also increase. Therefore, the energy exchanged by the batteries would represent a smaller portion of their total capacity and would have less impact on their life cycle.

For example, the case with 100 kW has double the ΔP_{max} available than the case with 50 kW. For the same value of

Δf_{max}, the value of P_{mav} does not scale by the same amount. If the total capacity of the batteries is assumed to be proportional to the available power, the impact on battery degradation would be different. On the other side, all scenarios with the same ΔP_{max} can be directly compared, as the assumption that the total capacity of the batteries is the same is fairly reasonable.

VII. CONCLUSION

In this paper, demand side contribution to frequency control in a weak electric power system with significant renewable generation has been evaluated using different metrics.

To be able to quantitatively compare the performance of different frequency control strategies, the authors have selected a set of conventional metrics and proposed a new one based on the density function of frequency. The new proposed metric allows a direct evaluation of the frequency behavior in the system, because it consists of a single numerical value that shows greater values as the frequency regulation presents a worse performance. This way, the comparison between different control strategies can be quantified and, in future developments, demand side response strategies can adapt to the changing conditions in a real electrical power system.

This new metric detects different types of frequency deviations, such as slow but significant variations around the rated value, or fast but small oscillations around a value other than the rated frequency, as shown in the example in section IV. The other presented metrics do not detect at least one of these cases, and would have to be used together to ensure the detection of frequency deviations of different types.

A total of 48 cases with different amounts of available power and response rates have been analyzed. The results indicate that, depending on the metric used, frequency behavior improves with more demand taking part in frequency control and higher response rates. However, no direct evidence for a hard limit on demand side participation has been detected. In a second phase, the impact on battery degradation caused by this frequency control strategy is compared, and it is shown that it is greater with higher response rates.

Regarding battery participation in frequency control, the main conclusion from this study is that there needs to be a trade-off between the contribution to frequency stability and battery degradation. This can be achieved by a combination of technical considerations, such as setting an appropriate value for Δf_{max}, and economical incentives, such as appropriate compensation for this participation.

DECLARATION OF COMPETING INTERESTS

The authors declare that they have no known competing financial interests or personal relationships that could have appeared to influence the work reported in this paper.

REFERENCES

[1] M. P. Jadhav and V. N. Kalkhambkar, "Frequency regulation by electric vehicle," in *Proc. Int. Conf. Current Trends Towards Converging Technol. (ICCTCT)*, Coimbatore, India, Mar. 2018, pp. 1–6, doi: 10.1109/ICCTCT.2018.8551055.

[2] F. Milano, F. Dorfler, G. Hug, D. J. Hill, and G. Verbic, "Foundations and challenges of low-inertia systems (invited paper)," in *Proc. Power Syst. Comput. Conf. (PSCC)*, Dublin, Ireland, Jun. 2018, pp. 1–25, doi: 10.23919/PSCC.2018.8450880.

[3] M. Nedd, J. Browell, K. Bell, and C. Booth, "Containing a credible loss to within frequency stability limits in a low-inertia GB power system," *IEEE Trans. Ind. Appl.*, vol. 56, no. 2, pp. 1031–1039, Mar. 2020, doi: 10.1109/TIA.2019.2959996.

[4] J. D. Glover and M. S. Sarma, *Power System Analysis and Design*, 3rd ed. Pacific Grove, CA, USA: Wadsworth, 2002.

[5] *Inertia and Rate of Change of Frequency (RoCoF)*, ENTSO-E, Brussels, Belgium, Dec. 2020.

[6] H. Bevrani, H. Golpîra, A. R. Messina, N. Hatziargyriou, F. Milano, and T. Ise, "Power system frequency control: An updated review of current solutions and new challenges," *Electr. Power Syst. Res.*, vol. 194, May 2021, Art. no. 107114, doi: 10.1016/j.epsr.2021.107114.

[7] D. Ochoa and S. Martinez, "Fast-frequency response provided by DFIG-wind turbines and its impact on the grid," *IEEE Trans. Power Syst.*, vol. 32, no. 5, pp. 4002–4011, Sep. 2017, doi: 10.1109/TPWRS.2016.2636374.

[8] R. H. Lasseter, "Smart distribution: Coupled microgrids," *Proc. IEEE*, vol. 99, no. 6, pp. 1074–1082, Jun. 2011, doi: 10.1109/JPROC.2011.2114630.

[9] U. Bose, S. K. Chattopadhyay, C. Chakraborty, and B. Pal, "A novel method of frequency regulation in microgrid," *IEEE Trans. Ind. Appl.*, vol. 55, no. 1, pp. 111–121, Jan. 2019, doi: 10.1109/TIA.2018.2866047.

[10] T. Jiang, P. Ju, C. Wang, H. Li, and J. Liu, "Coordinated control of air-conditioning loads for system frequency regulation," *IEEE Trans. Smart Grid*, vol. 12, no. 1, pp. 548–560, Jan. 2021, doi: 10.1109/TSG.2020.3022010.

[11] T. B. H. Rasmussen, Q. Wu, and M. Zhang, "Primary frequency support from local control of large-scale heat pumps," *Int. J. Electr. Power Energy Syst.*, vol. 133, Dec. 2021, Art. no. 107270, doi: 10.1016/j.ijepes.2021.107270.

[12] S. H. Tindemans, V. Trovato, and G. Strbac, "Decentralized control of thermostatic loads for flexible demand response," *IEEE Trans. Control Syst. Technol.*, vol. 23, no. 5, pp. 1685–1700, Sep. 2015, doi: 10.1109/TCST.2014.2381163.

[13] V. Trovato, I. M. Sanz, B. Chaudhuri, and G. Strbac, "Advanced control of thermostatic loads for rapid frequency response in Great Britain," *IEEE Trans. Power Syst.*, vol. 32, no. 3, pp. 2106–2117, May 2017, doi: 10.1109/TPWRS.2016.2604044.

[14] N. Neofytou, K. Blazakis, Y. Katsigiannis, and G. Stavrakakis, "Modeling vehicles to grid as a source of distributed frequency regulation in isolated grids with significant RES penetration," *Energies*, vol. 12, no. 4, p. 720, Feb. 2019, doi: 10.3390/en12040720.

[15] *Global EV Outlook 2021*, Int. Energy Agency, Paris, France, 2021.

[16] G. S. Ledva, E. Vrettos, S. Mastellone, G. Andersson, and J. L. Mathieu, "Managing communication delays and model error in demand response for frequency regulation," *IEEE Trans. Power Syst.*, vol. 33, no. 2, pp. 1299–1308, Mar. 2018, doi: 10.1109/TPWRS.2017.2725834.

[17] H. Liu, K. Huang, Y. Yang, H. Wei, and S. Ma, "Real-time vehicle-to-grid control for frequency regulation with high frequency regulating signal," *Protection Control Mod. Power Syst.*, vol. 3, no. 1, p. 13, Dec. 2018, doi: 10.1186/s41601-018-0085-1.

[18] W. Mendieta and C. A. Canizares, "Primary frequency control in isolated microgrids using thermostatically controllable loads," *IEEE Trans. Smart Grid*, vol. 12, no. 1, pp. 93–105, Jan. 2021, doi: 10.1109/TSG.2020.3012549.

[19] S. Nema, V. Prakash, and H. Pandzic, "Adaptive synthetic inertia control framework for distributed energy resources in low-inertia microgrid," *IEEE Access*, vol. 10, pp. 54969–54979, 2022, doi: 10.1109/ACCESS.2022.3177661.

[20] A. Khazali, N. Rezaei, H. Saboori, and J. M. Guerrero, "Using PV systems and parking lots to provide virtual inertia and frequency regulation provision in low inertia grids," *Electr. Power Syst. Res.*, vol. 207, Jun. 2022, Art. no. 107859, doi: 10.1016/j.epsr.2022.107859.

[21] J. M. Riquelme-Dominguez, F. D. P. García-López, and S. Martinez, "Power ramp-rate control via power regulation for storageless grid-connected photovoltaic systems," *Int. J. Electr. Power Energy Syst.*, vol. 138, Jun. 2022, Art. no. 107848, doi: 10.1016/j.ijepes.2021.107848.

[22] M. T. Muhssin, L. M. Cipcigan, N. Jenkins, S. Slater, M. Cheng, and Z. A. Obaid, "Dynamic frequency response from controlled domestic heat pumps," *IEEE Trans. Power Syst.*, vol. 33, no. 5, pp. 4948–4957, Sep. 2018, doi: 10.1109/TPWRS.2017.2789205.

[23] S. Nandkeolyar, R. K. Mohanty, and V. A. Dash, "Management of time-flexible demand to provide power system frequency response," in *Proc. Technol. Smart-City Energy Secur. Power (ICSESP)*, Bhubaneswar, India, Mar. 2018, pp. 1–4, doi: 10.1109/ICSESP.2018.8376678.

[24] U. Farooq and R. B. Bass, "Frequency event detection and mitigation in power systems: A systematic literature review," *IEEE Access*, vol. 10, pp. 61494–61519, 2022, doi: 10.1109/ACCESS.2022.3180349.

[25] T. Samad, E. Koch, and P. Stluka, "Automated demand response for smart buildings and microgrids: The state of the practice and research challenges," *Proc. IEEE*, vol. 104, no. 4, pp. 726–744, Apr. 2016, doi: 10.1109/JPROC.2016.2520639.

[26] J. J. Cuenca, E. Jamil, and B. Hayes, "State of the art in energy communities and sharing economy concepts in the electricity sector," *IEEE Trans. Ind. Appl.*, vol. 57, no. 6, pp. 5737–5746, Nov. 2021, doi: 10.1109/TIA.2021.3114135.

[27] *MATLAB and Simscape Power Systems Toolbox, Release 2018b*, MathWorks, Natick, MA, USA, 2018.

[28] D. Ochoa and S. Martinez, "Proposals for enhancing frequency control in weak and isolated power systems: Application to the wind-diesel power system of San Cristobal island-ecuador," *Energies*, vol. 11, no. 4, p. 910, Apr. 2018, doi: 10.3390/en11040910.

[29] L. Casasola-Aignesberger and S. Martinez, "Fast frequency oscillations detection in low inertia power systems with excessive demand-side response for frequency regulation," *Renew. Energy Power Qual. J.*, vol. 19, pp. 557–560, Sep. 2021, doi: 10.24084/repqj19.344.

[30] K. S. Hansen and G. C. Larsen. *Database of Wind Characteristics (DTU—Department of Wind Energy)*. Accessed: Sep. 1, 2022. [Online]. Available: http://winddata.com/

[31] D. D. Giudice, A. Brambilla, S. Grillo, and F. Bizzarri, "Effects of inertia, load damping and dead-bands on frequency histograms and frequency control of power systems," *Int. J. Electr. Power Energy Syst.*, vol. 129, Jul. 2021, Art. no. 106842, doi: 10.1016/j.ijepes.2021.106842.

[32] K. Dehghanpour and S. Afsharnia, "Electrical demand side contribution to frequency control in power systems: A review on technical aspects," *Renew. Sustain. Energy Rev.*, vol. 41, pp. 1267–1276, Jan. 2015, doi: 10.1016/j.rser.2014.09.015.

[33] F. Conte, M. C. di Vergagni, S. Massucco, F. Silvestro, E. Ciapessoni, and D. Cirio, "Synthetic inertia and primary frequency regulation services by domestic thermal loads," in *Proc. IEEE Int. Conf. Environ. Electr. Eng. IEEE Ind. Commercial Power Syst. Eur. (EEEIC/I CPS Europe)*, Genova, Italy, Jun. 2019, pp. 1–6, doi: 10.1109/EEEIC.2019.8783679.

[34] J. Guo, J. Yang, Z. Lin, C. Serrano, and A. M. Cortes, "Impact analysis of V2G services on EV battery degradation—A review," in *Proc. IEEE Milan PowerTech*, Milan, Italy, Jun. 2019, pp. 1–6, doi: 10.1109/PTC.2019.8810982.

LEO CASASOLA-AIGNESBERGER received the B.Sc. and M.Sc. degrees in industrial engineering from Universidad Politécnica de Madrid, Madrid, Spain, in 2016 and 2019, respectively, where he is currently pursuing the Ph.D. degree.

Since 2019, he has been a Teaching Assistant with the Electrical Engineering Department, Escuela Técnica Superior de Ingenieros Industriales, Universidad Politécnica de Madrid, while working on his Ph.D. thesis. His research interests include renewable energy generation, electrical power systems, microgrid control, and electrical markets.

SERGIO MARTÍNEZ (Senior Member, IEEE) was born in Madrid, Spain, in 1969. He received the M.Sc. degree in industrial engineering and the Ph.D. degree in electrical engineering from Universidad Politécnica de Madrid, Madrid, in 1993 and 2001, respectively.

He is currently an Associate Professor with the Department of Electrical Engineering, Escuela Técnica Superior de Ingenieros Industriales, Universidad Politécnica de Madrid. His research interests include electrical generation from renewable energy and the provision of ancillary services from electrical equipment connected to power systems through power electronics.